Article
Chinese Science Bulletin
Physical Chemistry
June 2012 Vol.57 No.16: 1964–1971
doi: 10.1007/s11434-012-5080-8

Theoretical characterization of electronic structures and properties of C–F···H–C pseudohydrogen bonds

YUAN Kun[1,2*], LIU YanZhi[1,2], LÜ LingLing[1,2], ZUO GuoFang[1,2], ZHU YuanCheng[1,2] & DONG XiaoNing[1,2]

[1] *College of Life-science and Chemistry, Tianshui Normal University, Tianshui 741001, China;*
[2] *Key Laboratory for New Molecular Materials Design and Function of Gansu Education Department, Tianshui 741001, China*

Received August 4, 2011; accepted December 9, 2011; published online March 30, 2012

The weak intermolecular interactions between 2-F-tetrahydrofuran and imidazole, pyrimidine, adenine, and guanine were studied theoretically using density functional B3LYP/6-311++G** and HF/6-311++G** methods. The results showed that both conventional N···H hydrogen bond and C–F···H–C pseudohydrogen bond (PHB) structures coexist in the four complexes. The weak intermolecular interaction energies indicate that the relative stabilities of the four complexes are in the order guanine···F > imidazole···F > adenine···F > pyrimidine···F. The characteristics of the four PHBs were determined using geometry optimizations, stretching vibrational frequencies, and natural bond orbital and electron density topological properties calculations. The most important result is that the F group of 2-F-tetrahydrofuran can activate the C–H to accept electrons from another molecule, and C–F···H–C PHB formation is relatively favorable.

weak interaction, pseudohydrogen bond, electronic structure, electron density topological property

Citation: Yuan K, Liu Y Z, Lü L L, et al. Theoretical characterization of electronic structures and properties of C–F···H–C pseudohydrogen bonds. Chin Sci Bull, 2012, 57: 1964–1971, doi: 10.1007/s11434-012-5080-8

Most biological phenomena are directly or indirectly related to supermolecular compounds. Such compounds are based on weak intermolecular interactions. Weak intermolecular interactions are important in the fields of biological molecular recognition [1–3], molecular and crystal engineering [4], formation of molecular clusters [5,6], chemical reactions [7], materials design, and molecular self-assembly [8,9]. Typical weak intermolecular interactions reported in the literature are hydrogen bonds, halogen bonds, and lithium bonds. Hydrogen bonds have long been of interest to chemists, and many theoretical and experimental studies have been reported. Recently, to obtain materials with novel light, electrical, or magnetic properties, the orientation properties of hydrogen bonds have been used in crystal engineering, and structures or functional units have been assembled in specific ways desired by researchers.

Because many strong hydrogen-bond receptors exist in aqueous solutions, organic fluorine compounds generally can not be used as hydrogen-bonding receptors [10,11]. Fluorine (F) is not as good a hydrogen-bond receptor (electron donor) as oxygen (O) is; F generally bonds with only one atom or group in a molecule, whereas O bonds with two atoms or groups. So, in some chemical environments, for example, biological systems, F has advantages over O as a hydrogen-bonding receptor in terms of space geometry. Compared with other common hydrogen-bond donors such as –OH and $–NH_2$ groups, –C–H is a weak hydrogen-bond donor (electron receptor). However, when –C–H acting as a hydrogen-bond donor interacts with the F functional group of another molecule, the F group may increase the activity of the C–H (hydrogen-bond donor) group, forming a relatively stable weak intermolecular interaction.

Heterocyclic compounds exist widely in natural biological macromolecules (such as proteins and nucleic acids);

*Corresponding author (email: yuankun@tsnc.edu.cn)

their biological activity depends to a great extent on the molecular space configuration, and these molecular space configurations are closely related to hydrogen-bond structures. Pallan found C–F···H–N base pairs with short action distances in a complex of difluorine-substituted toluene··· adenine [12]. This type of interaction was tested in aqueous solutions, which contained a large number of other strong hydrogen-bond receptors; the interaction energy was very small, and insufficient to prove the existence of F–C···H–N hydrogen bonds. However, F–C···H–R weak interactions in nucleobase derivatives had been reported earlier [13–17] and defined as pseudohydrogen bonds (PHBs) by Bergstrom et al. [18]. Watts et al. [19] made a detailed study of the arabinonucleic acid (ANA), ribonucleic acid (RNA) duplex (AR) and 2′F-ANA·RNA duplex (FR) experimentally and using theoretical calculations. It was found that a PHB structure was formed between the 2′F of the tetrahydrofuran ring and H6/H8 of the aromatic ring in the FR duplex (Figure 1(a)). However, there was no HO···H–C hydrogen-bond formation between the –OH of the ANA and H6/H8 of RNA in the AR duplex (Figure 1(b)) because of steric effects. In early 2011, Anzahaee et al. [20] studied 2′F-ANA C–F···H–C PHBs in aqueous solutions and found experimental evidence of PHBs; applications to the rational design of oligonucleotides with high binding affinities were also discussed. There have as yet been no reports of investigations of the electronic structures and properties of C–F···H–C PHBs. In this study, several common and important small biomolecules, namely imidazole, pyrimidine, adenine, and guanine, were investigated; the PHB weak interactions between 2-F-tetrahydrofuran and these small biomolecules were analyzed, and the electronic behaviors and thermodynamic stabilities of the PHB complexes were revealed using quantum chemistry calculations.

1 Computational details

All the monomers and complexes were optimized using the density functional B3LYP (Becke, three-parameter, Lee-Yang-Parr) and HF (Hartree-Fock) methods. Harmonic frequency analyses were performed at the same levels to confirm that these structures were local minima on the energy surfaces. The interaction energies were corrected with the basis set superposition error (BSSE). The BSSE was evaluated using the counterpoise method of Boys and Bernardi [21]. Because of the nature of intermolecular interactions, the accuracy of the calculation results has a close relationship with the primary functions. The basis sets chosen must include polarized and dispersion functions. Previous studies have demonstrated that the introduction of polarized and dispersion functions could significantly decrease the BSSE [22]. The 6-311++G** basis set was therefore adopted for all atoms. Natural bond orbital (NBO) theory [23] and Bader's atoms-in-molecules (AIM) theory [24] were used to analyze the electronic behaviors and electron density topological properties, respectively. NBO calculations were carried out using the NBO 5.0 package [25]. All other calculations were performed using the Gaussian 03 program [26].

2 Results and discussion

2.1 Geometric configurations and PHB structures

The optimized geometric configurations on the potential surfaces of the monomers and C–F···H–C complexes at the B3LYP//HF/6-311++G** computational levels are shown in Figure 2. The frequency analysis shows that all the configurations are stable points on the potential surfaces of the complexes. Some important bond length parameters obtained at the B3LYP/6-311++G** computational levels are also shown. As shown in Figure 2, in the four complexes, C–F···H–C PHBs were formed via the C1–H1 groups of imidazole, pyrimidine, adenine, and guanine as the electron acceptors (PHB donors) and the F group of 2-F-tetrahydrofuran as the electron donor (PHB acceptor). Simultaneously, conventional N···H2–C2 hydrogen bonds were formed via the N atoms of the four biomolecules as electron donors

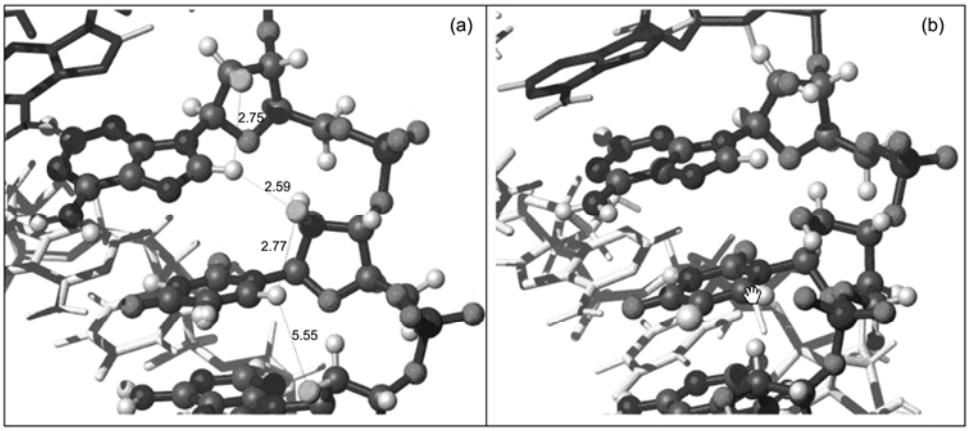

Figure 1 F2′···H8 interactions in FR (a) and AR (b) [19].

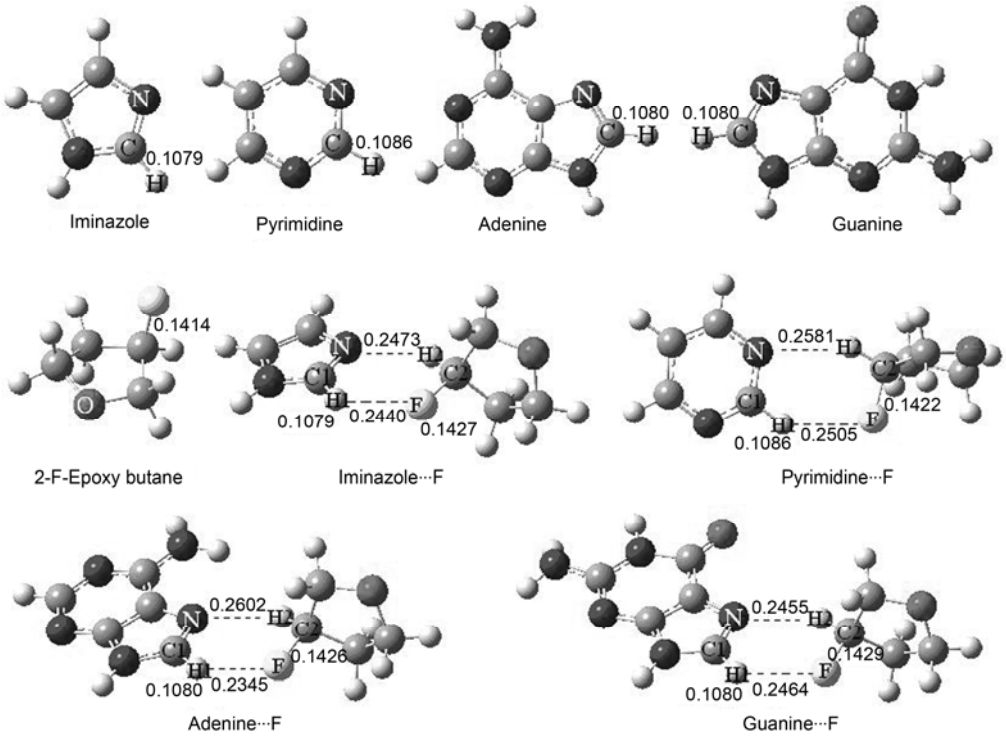

Figure 2 Geometries (nm) of the monomers and four complexes calculated at B3LYP//HF/6-311++G** levels.

(hydrogen-bond acceptor) and the H2–C2 group of 2-F-tetrahydrofuran as the electron acceptor (hydrogen-bond donor). Two molecules in the complexes are therefore combined by one PHB and one conventional hydrogen-bond interaction. The six atoms labeled in Figure 2 as NC1H1-FC2H2 are in the same plane, i.e. a planar six-atom ring structure with thermodynamic stability is formed at the binding region of the two molecules. The van der Waals and covalent radii are important factors in investigating the geometric structure. If the distance between two atoms is obviously less than the sum of their van der Waals radii, but larger than the sum of their covalent radii, a certain degree of weak interaction which is stronger than van der Waals forces exists between the two atoms, for example, a hydrogen bond or halogen bond. In this study, the F···H1 distances in the complexes are in the range 0.2345–0.2505 nm. The experimental values of the van der Waals and covalent radii of an H atom are 0.120 and 0.037 nm, respectively, and those of an F atom are 0.147 and 0.064 nm, respectively. It is therefore clear that the atomic pair distances of the two atoms directly involved in the PHB formation are less than the sums of their van der Waals radii but larger than the sums of their covalent radii. It can be concluded that there is a degree of weak interaction, which is stronger than van der Waals forces, between the F···H1 atoms. Of course, the van der Waals and covalent radii of the atoms directly involved in the formation of conventional N···H2–C2 hydrogen bonds also obey this rule.

In conventional hydrogen-bond structures, the bond length of the hydrogen-bond donor (X–H, X=N, O, S, etc.) usually increases to a certain degree, but in the C–F···H–C PHB structures in the present study, the C1–H1 bond length did not change as a result of complex formation. This is one of the characteristics of a PHB which differs from those of conventional hydrogen bonds. This is probably related to electronic effects before and after forming the PHB structure; this will be discussed below. It is interesting that the C2–F bond length in the 2-F-tetrahydrofuran monomer, which is 0.1414 nm, increased significantly after formation of the PHB complexes; for example, the C2–F bond in the guanine···F complex was 0.0015 nm longer than that in the monomer. The increased C2–F bond length results in a red-shift of the stretching vibrational frequency. In summary, the C2–F (the group closely related to the electron donor, i.e. the F group of 2-F-tetrahydrofuran, of the PHB structure) bond length increases, and its stretching vibrational frequency is red-shifted. However, in a conventional hydrogen bond, what presents increasing of bond length and red-shift of stretch vibrational frequency is often the electron acceptor group. This is another way in which PHBs differ from conventional hydrogen bonds.

2.2 Interaction energies and frequency analyses

Examining interaction energies is a powerful approach to estimating the strength of a weak interaction. The total interaction energies (ΔE) and BSSE corrected energies (ΔE_{CP}) of the four complexes at the B3LYP/6-311++G** and HF/6-311++G** levels are listed in Table 1. It should be noted that the energies listed in Table 1 are not those of pure PHB

Table 1 Interaction energies (kJ mol^{-1}) of the four complexes at the B3LYP//HF/6-311++G** levels

Complexes	B3LYP/6-311++G**			HF/6-311++G**		
	ΔE	BSSE	ΔE_{CP}	ΔE	BSSE	ΔE_{CP}
Imidazole···F	−14.35	1.35	−13.00	−13.34	0.74	−12.60
Pyrimidine···F	−8.73	1.52	−7.21	−7.86	1.76	−6.10
Adenine···F	−11.57	1.51	−10.06	−11.01	2.11	−8.90
Guanine···F	−16.52	1.66	−14.86	−16.10	2.82	−13.28

interactions because C–F···H–C PHBs and conventional N···H–C hydrogen bonds exist simultaneously in the four complexes. As shown in Table 1, before and after BSSE correction using the counterpoise method, ΔE and ΔE_{CP} values obtained by the HF method are always smaller than those obtained by the B3LYP method, but the energies obtained by the two computational methods do not differ greatly. The absolute values of the BSSEs, obtained using either the HF or B3LYP method, are relatively small, not more than 3 kJ mol^{-1}, especially at the B3LYP/6-311++G** level, and the maximum BSSE is only 1.66 kJ mol^{-1}. However, it is necessary to perform a counterpoise correction to obtain accurate interactions. Additionally, as can be seen from the relative sizes of the energies (ΔE and ΔE_{CP}) obtained by the HF and B3LYP methods, the tendencies of the energy changes are consistent. For example, the ΔE_{CP} values of the four complexes at the B3LYP/6-311++G** level are −13.00, −7.21, −10.06, and −14.86 kJ mol^{-1}, and the corresponding values at the HF/6-311++G** level are −12.06, −6.10, −8.90, and −13.28 kJ mol^{-1}. It can therefore be inferred that the relative stabilities of the four complexes decrease in the order guanine···F > imidazole···F > adenine···F > pyrimidine···F.

The correlation between ΔE_{CP} and changes in the C2–F bond length (Δd_{C2-F}) at the B3LYP/6-311++G** computational level is shown in Figure 3. After formation of the complexes, the greater the increase in the C2–F bond length, the larger (more negative) ΔE_{CP} is. In fact, the ΔE_{CP} values

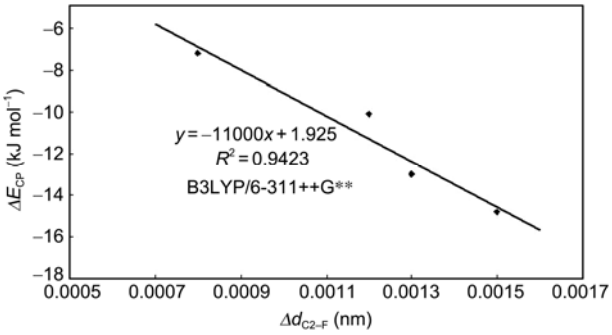

Figure 3 The linear relationship between Δd_{C2-F} and ΔE_{CP}.

of the four complexes correlate linearly correlated to Δd_{C2-F}, and the relevant equation is $y = -11000x + 1.925$ ($R^2 = 0.9423$). There is therefore an obvious correlation between the bond length of C2–F, which is closely related to the C–F···H–C PHB structure, and the intermolecular interaction energy. So, although C–F···H–C PHBs and conventional N···H–C hydrogen bonds coexist in the four complexes, it can be concluded that the contributions of the C–F···H–C PHBs to the intermolecular interaction energies and stabilities of the complexes are more significant than those of conventional N···H–C hydrogen bonds.

The stretching vibrational frequencies, IR intensities, and frequency shifts of the C1–H1 and C2–F bonds of the monomers and complexes calculated at the B3LYP/6-311++G** and HF/6-311++G** levels are listed in Table 2.

Table 2 Stretching vibrational frequencies (cm^{-1}), frequency shifts (cm^{-1}, in italics in brackets), and IR intensities (km mol^{-1}, in regular type in brackets) of the C1–H1 and C2–F bonds

Compound	Parameter [a)]	B3LYP/6-311++G**	HF/6-311++G**
Imidazole	υ_{C1-H1}	3244.5 (0.7)	3397.7(5.4)
Pyrimidine	υ_{C1-H1}	3167.6 (13.8)	3347.5(20.6)
Adenine	υ_{C1-H1}	3240.2 (0.2)	3397.9(1.6)
Guanine	υ_{C1-H1}	3242.9 (0.3)	3402.7(1.4)
2-F-Tetrahydrofuran	υ_{C2-F}	832.6 (33.2)	914.3(28.8)
Imidazole···F	υ_{C1-H1}, υ_{C2-F}	3247.4(10.2, *2.9*), 821.5(38.5, *−11.1*)	3407.2(2.9, *9.5*), 909.8(33.7, *−4.5*)
Pyrimidine···F	υ_{C1-H1}, υ_{C2-F}	3179.5(1.2, *11.9*), 825.4(33.1, *−7.2*)	3361.6(7.2, *14.1*), 911.2(29.4, *−3.1*)
Adenine···F	υ_{C1-H1}, υ_{C2-F}	3242.0(18.1, *1.8*), 820.2(36.4, *−12.4*)	3409.1(4.7, *11.2*), 908.5(31.4, *−4.8*)
Guanine···F	υ_{C1-H1}, υ_{C2-F}	3245.9(10.6, *3.0*), 818.7(38.4, *−13.9*)	3411.8(1.6, *9.1*), 910.3(32.3, *−4.0*)

a) For atom numbers, see Figure 2.

The C1–H1 (PHB donor) bond lengths are the same before and after formation of the complexes, but the stretching vibrational frequencies of the C1–H1 bonds show a small blue-shift. However, the stretching vibrational frequency of the hydrogen-bond donor usually shows an obvious red-shift in a conventional hydrogen bond. The stretching vibrational frequency of the C2–F bond in the 2-F-tetrahydrofuran moiety tends to red-shift after complex formation. This is consistent with increases in the C2–F bond lengths. Furthermore, as shown in Figure 4, the red-shift values ($\Delta\upsilon_{C2-F}$) of the stretching vibrational frequencies of the C2–F bonds are linearly correlated to variations in the C2–F bond lengths (Δd_{C2-F}); the relevant equation is $y=-9384.5x+0.1615$ ($R^2=0.9369$). In fact, the relationship between $\Delta\upsilon_{C2-F}$ and the C2–F bond length (d_{C2-F}) is also linear ($y=-9383.6x+1327.1$, $R^2=0.9369$), i.e. longer d_{C2-F} values and larger Δd_{C2-F} values correspond to larger values of $\Delta\upsilon_{C2-F}$. Table 2 also shows that, except for the IR intensity of the C1–H1 bond of the pyrimidine moiety, the C2–F and C1–H1 bond lengths all increased after complex formation. The IR intensity (I) is directly proportional to the square of the partial derivative of the correlative atom displacement (r) with respect to the electric dipole moment (μ), which can be described as $I \propto |d\mu/dr_{X-H}|^2$, and the existence of PHBs in the complexes caused further polarization of the C2–F bonds, with large dipole moments, so the IR intensity increased.

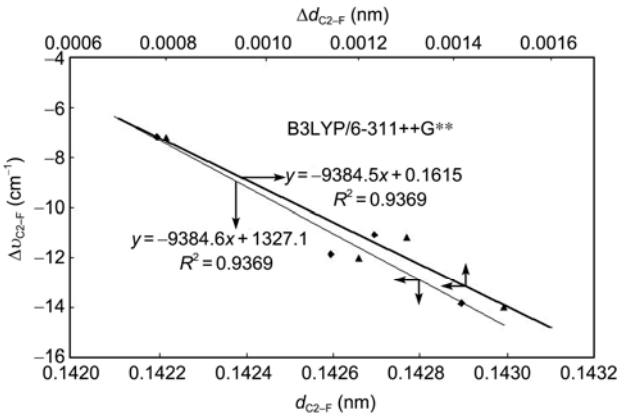

Figure 4 Linear relationships between d_{C2-F} and Δd_{C2-F}, and d_{C2-F} and $\Delta\upsilon_{C2-F}$.

2.3 NBO analysis and charge transfer

For a better understanding of the mechanism of PBH complex formation, NBO analyses were performed for the monomers and complexes at the B3LYP/6-311++G** level, and the corresponding results are listed in Table 3. As shown in Table 3, there are three main types of charge transfer between NBOs in the four PHB complexes. These are LP1(F)→BD*(C1–H1), LP3(F)→BD*(C1–H1), and LP(N)→BD*(C2–H2); three-dimensional images of the first two are given in Figure 5(a-1), (b-1), (c-1), and (d-1); they are related to the charge transfer behavior of the C–F···H–C PHB structures in the four complexes. Three-dimensional images of the third type of charge transfer, i.e., between LP(N) and BD*(C2–H2), are shown in Figure 5(a-2), (b-2), (c-2), and (d-2); these are related to the charge transfer behavior of the conventional N···H–C hydrogen bond structures in the four complexes. There are three lone pairs of electrons. The first and third pairs are involved in the formation of PHBs, but the contributions of these two lone pairs are different. Because of the larger donor–acceptor orbital interaction stabilization energy ($E_{ij}^{(2)}$) between LP3(F) and the BD*(C1–H1) orbital, the contribution of LP3(F) is larger than the that of LP1(F). The second lone pair of electrons, LP2(F), with s(0.05%)p99.99(99.95%) hybridization of the F atom, did not participate in PHB

Table 3 Analyses of natural bond orbitals and charge transitions at the B3LYP/6-311++G** level

Complexes	Elector donor [a]/type	Elector acceptor [b]	$E^{(2)}$ (kcal mol^{-1})	Δq (e) BD* (C–H)	Δ_{NBO} (e)
Imidazole···F	LP1(F)/s(71.8%)p$^{0.39}$(28.2%)	BD*(C1–H1)	0.21	0.0004	0.006
	LP3(F)/s(2.1%)p$^{47.1}$(97.9%)	BD*(C1–H1)	0.75		
	LP(N)/s(33.6%)p$^{1.97}$(66.3%)	BD*(C2–H2)	2.31	0.0020	
Pyrimidine···F	LP1(F)/s(72.2%)p$^{0.39}$(27.8%)	BD*(C1–H1)	0.12	–0.0007	0.004
	LP3(F)/s(1.6%)p$^{62.0}$(98.4%)	BD*(C1–H1)	0.58		
	LP(N)/s(29.6%)p$^{2.38}$(70.3%)	BD*(C2–H2)	1.66	0.0014	
Adenine···F	LP1(F)/s(72.1%)p$^{0.41}$(28.9%)	BD*(C1–H1)	0.30	0.0009	0.002
	LP3(F)/s(2.6%)p$^{37.5}$(97.4%)	BD*(C1–H1)	1.16		
	LP(N)/s(33.8%)p$^{1.95}$(66.1%)	BD*(C2–H2)	1.46	0.0012	
Guanine···F	LP1(F)/s(71.6%)p$^{0.40}$(28.4%)	BD*(C1–H1)	0.21	0.0000	0.005
	LP3(F)/s(2.2%)p$^{45.42}$(97.8%)	BD*(C1–H1)	0.59		
	LP(N)/s(33.7%)p$^{1.96}$(66.2%)	BD*(C2–H2)	2.27	0.0012	

a) LPi(i=1, 2, 3) presents the lone electrons; b) BD* presents anti-bond orbital. For atom numbers, see Figure 2.

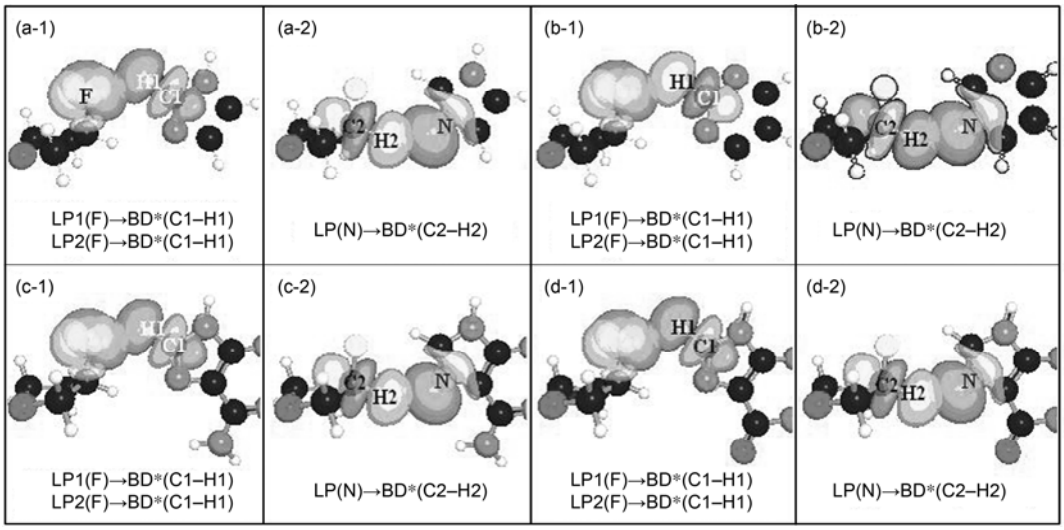

Figure 5 Three-dimensional images of the main orbital interactions in the four complexes.

formation. Although LP1(F) and LP3(F) offer electrons to BD*(C1–H1), there is no obvious increase in the electronic population of the BD*(C1–H1) orbital. In fact, the electronic population of the BD*(C1–H1) orbital basically remains unchanged. This point can be regarded as the third way in which PHBs differ from conventional hydrogen bonds. In the four complexes, the largest increase in the electronic population (Δq) of the BD*(C1–H1) orbital is seen in the adenine···F complex, but the increase is only 0.0009 e. This is consistent with the C1–H1 bond length being the same before and after complex formation. As a result of these charge transfer interactions between NBOs and the rehybridization of the related atoms, the NBO charge population of each moiety in the complexes is redistributed. In summary, the NBO charge transfers (Δ_{NBO}) are 0.006, 0.004, 0.002, and 0.005 e in the imidazole···F, pyrimidine···F, adenine···F, and guanine···F complexes, respectively.

As mentioned in the introduction, –C–H is a hydrogen-bond donor (electron receptor). However, when –C–H, which is a weak hydrogen-bond donor, interacts with the F group of another molecule, the donor activity of the –C–H would be increased by the F group, thus a relatively stable weak intermolecular interaction system will be formed. This can be proved via NBO analysis. The difference between the electronegativities of C and H is small, so the polarity of a C–H covalent bond is very weak, and it is hard to form the bare proton needed for a hydrogen-bond donor. However, the electronegativity of the C atom is related to its hybridization type. Generally, the higher the s content of the hybrid atomic orbital, the stronger the electronegativity, i.e., when the s content of the C atom hybrid orbital is sufficient, the C–H group is a better hydrogen-bond donor. The hybridization types of the C1 atoms of the PHB donor (C1–H) orbitals and those of the F of the PHB acceptor and C2 atoms before and after complex formation are listed in Table 4. As shown in Table 4, compared with the monomers, the s contents of the C1 atom hybrid orbital of the four C1–H1 bond orbitals all increased after formation of the four PHBs. It is thus clear that the F group, the electron donor, can indeed

Table 4 Hybridizations of the related atoms, C1, F, and C2, before and after PHB formation

Compound	Bond orbital	Hybrids of C1	Hybrids of C2	Hybrids of F
Imidazole	C1–H1	$s(34.9\%)p^{1.87}(65.1\%)$	–	–
Pyrimidine	C1–H1	$s(30.9\%)p^{2.23}(69.1\%)$	–	–
Adenine	C1–H1	$s(34.4\%)p^{1.91}(65.6\%)$	–	–
Guanine	C1–H1	$s(34.8\%)p^{1.88}(65.2\%)$	–	–
2-F-Tetrahydrofuran	C2–F	–	$s(18.0\%)p^{4.53}(81.6\%)$	$s(26.5\%)p^{2.78}(73.5\%)$
Imidazole···F	C1–H1, C2–F	$s(35.5\%)p^{1.82}(64.5\%)$	$s(17.2\%)p^{4.80}(82.5\%)$	$s(26.1\%)p^{2.83}(73.8\%)$
Pyrimidine···F	C1–H1, C2–F	$s(31.5\%)p^{2.17}(68.44\%)$	$s(17.3\%)p^{4.74}(82.3\%)$	$s(26.2\%)p^{2.82}(73.8\%)$
Adenine···F	C1–H1, C2–F	$s(35.1\%)p^{1.85}(64.9\%)$	$s(17.5\%)p^{4.69}(82.1\%)$	$s(26.2\%)p^{2.82}(73.8\%)$
Guanine···F	C1–H1, C2–F	$s(35.4\%)p^{1.83}(64.6\%)$	$s(17.3\%)p^{4.78}(82.4\%)$	$s(26.1\%)p^{2.83}(73.8\%)$

increase the electron-acceptor activity of the –C–H group, and thus further formation of PHB structures is easy. As discussed in the section on geometric configuration and PHB structure, the F–C2 bond after PHB complex formation was significantly longer than that in the 2-F-tetrahydrofuran monomer. This change can also be explained by the composition of the hybrid atomic orbital of the C2 atom bound to the F atom. Table 4 also shows that the s contents of the hybrid atomic orbitals of the F and C2 atoms in the PHB complexes were all to some degree less than those of the hybrid atomic orbitals of the F and C2 atoms in the 2-F-tetrahydrofuran monomer. The covalent bond formed between two atoms with small s contents in the hybrid atomic orbital is relatively weak, and therefore the corresponding bond length is large.

2.4 Electron density topological properties

The electronic structures of the PHBs can be described by the scalar field electron density ($\rho(r)$) topological properties of the corresponding critical points. The topological properties of $\rho(r)$ can be further indicated by the numbers and categories of the critical points. A critical point is a spatial position where the first derivative of $\rho(r)$ is zero. The critical point type can be defined according to its curvature, obtained by calculating the second derivative of $\rho(r)$. The Hessian matrix of the electron density is composed of nine secondary derivatives of $\rho(r)$ in three dimensions. The three eigenvalues (λ_1, λ_2, and λ_3) can be acquired by performing a diagonalized operator on the Hessian matrix. The sum of the three eigenvalues is equal to the Laplacian of the electron density ($\nabla^2\rho(r)=\lambda_1+\lambda_2+\lambda_3$). If two of the eigenvalues are negative and the other is positive, the corresponding critical point is designated as the bond critical point (BCP) and marked as (3, −1), indicating the linkage between the two atoms.

According to Bader's AIM theory [24,27], the electron density topological properties of a molecule depend on the electron density gradient vector field and $\nabla^2\rho(r)$. In general, the electron density of a BCP ($\rho(r_c)$) is related to the strength of the bond: the larger the value of $\rho(r_c)$, the stronger the bond, and the smaller the $\rho(r_c)$ value, the weaker the bond. The $\nabla^2\rho(r)$ of the BCP reflects the characteristics of the bond. If $\nabla^2\rho(r_c)<0$, the BCP charges will be concentrated, and the more negative $\nabla^2\rho(r_c)$ is, the more covalent the bond is; if $\nabla^2\rho(r_c)>0$, the BCP charges will be dispersed, and the more positive $\nabla^2\rho(r_c)$ is, the more ionic the bond is.

The electron density topological properties of the PHB and conventional hydrogen bond critical points in the four complexes are listed in Table 5. The three eigenvalues of the electron density Hessian matrices of F···H1 and N···H2 are "one positive and two negative". The critical points between the F···H1 and N···H2 atom pairs therefore belong to the type BCP. The $\rho(r)$ values of F···H1 and N···H2 in the four complexes are smaller than 0.011 a.u. This indicates that the C2–F···H1–C1 PHB and conventional N···H2 hydrogen bond interactions in the complexes are weak; this is in good agreement with the calculation results for the interaction energies. The $\nabla^2\rho(r)$ of the corresponding critical points are all small negative values; this indicates that these types of weak interaction are more electrostatic than covalent. It is notable that the $\nabla^2\rho(r)$ values of the C2–F··· H1–C1 PHBs in the four complexes are close to those of conventional N···H2 hydrogen bonds. This indicates that the covalent and ionic properties of the C2–F···H1–C1 PHBs are basically equal to those of conventional N···H2 hydrogen bonds. The ellipticity, ε, is defined as λ_1/λ_2-1, where λ_1 and λ_2 are two eigenvalues of the Hessian matrix of electron density. The ε value provides a measure of the σ or π character of a bond. In general, the lower ε is, the stronger the σ character, and, conversely, the higher ε is, the stronger the π character. Here, all the ε values are small, and those for the C2–F···H1–C1 PHBs are always smaller than those for conventional N···H2 hydrogen bonds; this indicates that the C2–F···H1–C1 PHBs have stronger σ characters than conventional N···H2 hydrogen bonds have, i.e. C2–F···H1–C1 PHBs have higher orbital "bond axis" symmetry.

Table 5 Electron density topological properties of pseudohydrogen bond and conventional hydrogen bond critical points

Compound	Atom pair [a)]	$\rho(r_c)$ (a.u.)	λ_1	λ_2	λ_3	$\nabla^2\rho(r_c)$ (a.u.)	ε
Imidazole···F	F···H1	0.0083	–0.00852	–0.00824	0.04799	0.03123	0.03295
	N···H2	0.0106	–0.01014	–0.00958	0.05081	0.03110	0.05885
Pyrimidine···F	F···H1	0.0072	–0.00734	–0.00703	0.04096	0.02659	0.04481
	N···H2	0.0090	–0.00836	–0.00792	0.04132	0.02504	0.05508
Adenine···F	F···H1	0.0100	–0.01088	–0.01042	0.05840	0.03710	0.04440
	N···H2	0.0082	–0.00720	–0.00679	0.03734	0.02335	0.06096
Guanine···F	F···H1	0.0080	–0.00799	–0.00779	0.04611	0.03033	0.02502
	N···H2	0.0109	–0.01072	–0.01008	0.05384	0.03305	0.06364

a) For atom numbers, see Figure 2.

3 Conclusions

The weak intermolecular interactions in 2-F-tetrahydrofuran···M (M = imidazole, pyrimidine, adenine, and guanine) complexes were examined theoretically using density functional B3LYP/6-311++G** and HF/6-311++G** methods. The results showed that both conventional N···H hydrogen bonds and C–F···H–C PHB structures coexist in the four complexes. The C–F···H–C PHBs have the following four characteristics which are different from those of conventional hydrogen bonds. (1) In conventional hydrogen-bond structures, the bond length of the hydrogen-bond donor (X–H, X=N, O, S, etc.) usually increases to a certain degree, but in the C–F···H–C PHB structures, the C1–H1 (PHB donor) bond length is the same before and after complex formation. (2) The PHB electron-donor (C2–F) bond is elongated, and its stretching vibrational frequency is red-shifted, whereas in a conventional hydrogen bond, this behavior is usually shown by the electron-acceptor group. (3) The electronic population of the BD*(C1–H1) (electron acceptor) orbital basically remains unchanged. The activity of –C–H as an electron acceptor is increased by the F group of 2-F-tetrahydrofuran. (4) The covalent and ionic properties of the C2–F···H1–C1 PHBs are basically equal to those of conventional N···H2 hydrogen bonds, but the C2–F···H1–C1 PHBs have higher orbital "bond axis" symmetry.

This work was supported by the Key Project of the Chinese Ministry of Education (211189), the National Natural Science Foundation of China (51063006), and the "QingLan" Talent Engineering Funds of Tianshui Normal University.

1 Jiao T F, Liu M H. Supramolecular asemblies and molecular recognition of amphiphilic schiff bases with barbituric acid in organized mMolecular films. J Phys Chem B, 2005, 109: 2532–2539
2 Jesus V, Surya K D, Chen L H, et al. Development of paramagnetic probes for molecular recognition studies in protein kinases. J Med Chem, 2008, 51: 3460–3465
3 Xi L, Peng Y H, Ren J S, et al. Carboxyl-modified single-walled carbon nanotubes selectively induce human telomeric i-motif formation. Proc Natl Acad Sci USA, 2006, 103: 19658–19663
4 Dastidar P. Supramolecular gelling agents: Can they be designed? Chem Soc Rev, 2008, 37: 2699–2715
5 Lehmann S B C, Spickermann C, Kirchner B. Quantum cluster equilibrium theory applied in hydrogen bond number studies of water. 1. Assessment of the quantum custer equilibrium model for liquid water. J Chem Theory Comput, 2009, 5: 1640–1649
6 Nguyen T N V, Hughes S R, Peslherbe G H. Microsolvation of the sodium and iodide ions and their ion pair in acetonitrile clusters: A theoretical study. J Phys Chem B, 2008, 112: 621–635
7 Mohammed G S, Bojan D, Lee J S, et al. Thermodynamics of halogen bonding in solution: Substituent, structural, and solvent effects. J Am Chem Soc, 2010, 132: 1646–1653
8 Mu Z C, Shu L J, Fuchs H, et al. Two dmensional chiral networks emerging from the aryl–F···H hydrogen-bond-driven self-assembly of partially fluorinated rigid molecular structures. J Am Chem Soc, 2008, 130: 10840–10841
9 Lv F Z, Peng Z H, Zhang L L, et al. A new type of hydrogen-bonded LBL photoalignment film for liquid crystal (in Chinese). Acta Phy-Chim Sin, 2009, 25: 273–277
10 Howard J A K, Hoy V J, OHagan D, et al. How good is fluorine as a hydrogen bond acceptor? Tetrahedron, 1996, 52: 12613–12622
11 Dunitz J D. Organic fluorine: Odd man out. ChemBioChem, 2004, 5: 614–621
12 Pallan P S, Egli M. Pairing geometry of the hydrophobic thymine analogue 2,4-difluorotoluene in duplex DNA as analyzed by X-ray crystallography. J Am Chem Soc, 2009, 131: 12548–12549
13 Bats J W, Parsch J, Engels J W. 1-deoxy-1-(4-fluorophenyl)-beta-D-ribofuranose, its hemihydrate, and 1-deoxy-1-(2,4-difluorophenyl)-beta-D-ribofuranose: Structural evidence for intermolecular C–H···F–C interactions. Acta Crystallogr Sect C–Cryst Struct Commun, 2000, 56: 201–205
14 Parsch J, Engels J W. C–F···H–C hydrogen bonds in ribonucleic acids. J Am Chem Soc, 2002, 124: 5664–5672
15 Frey J A, Leist R, Leutwyler S. Hydrogen bonding of the nucleobase mimic 2-pyridone to fluorobenzenes: An *ab initio* investigation. J Phys Chem A, 2006, 110: 4188–4195
16 Sun Z, McLaughlin L W. Probing the nature of three-centered hydrogen bonds in ligand-DNA interactions in the minor groove. J Am Chem Soc, 2007, 129: 12531–12536
17 Koller A N, Bozilovic J, Engels J W, et al. Aromatic N versus aromatic F: Bioisosterism discovered in RNA base pairing interactions leads to a novel class of universal base analogs. Nucleic Acids Res, 2010, 38: 3133–3146
18 Bergstrom D E, Swartling D J, Wisor A, et al. Evaluation of thymidine, dideoxythymidine and fluorine substituted deoxyribonucleoside geometry by the Mindo/3 technique: The effect of fluorine substitution on nucleoside geometry and biological activity. Nucleosides Nucleotides, 1991, 10: 693–697
19 Watts J K, Martin-Pintado N, Gomez-Pinto I, et al. Differential stability of 2'F-ANA*RNA and ANA*RNA hybrid duplexes: Roles of structure, pseudohydrogen bonding, hydration, ion uptake and flexibility. Nucleic Acids Res, 2010, 38: 2498–2511
20 Anzahaee M Y, Watts J K, Alla N R, et al. Energetically important C–H···F–C pseudohydrogen bonding in water: Evidence and application to rational design of oligonucleotides with high binding affinity. J Am Chem Soc, 2011, 133: 728–731
21 Boys S F, Bernardi F. Calculation of small molecular interactions by differences of separate total energies. Some procedures with reduced errors. Mol Phy, 1970, 19: 553–556
22 King B F, Weinhold F. Structure and spectroscopy of $(HCN)_n$ clusters: Cooperative and electronic delocalization effects in C–H···N hydrogen bonding. J Chem Phys, 1995, 103: 333–347
23 Reed A E, Curtiss L A, Weinhold F. Intermolecular interactions from a natural bond orbital, donor-acceptor viewpoint. Chem Rev, 1988, 88: 899–926
24 Bader R F W. Atoms in Molecules: A Quantum Theory. New York: Clarendon Press, 1990
25 Glendening E D, Badenhoop J K, Reed A E, et al. Natural bond orbital program. Version 5.0. Madison, WI: Theoretical Chemistry Institute, University of Wisconsin, 2001
26 Frisch M J, Trucks G W, Schlegel H B, et al. Gaussian 03 E. 01. Pittsburgh PA: Gaussian Inc, 2004
27 Bader R F W. A quantum theory of molecular structure and its applications. Chem Rev, 1991, 91: 893–928